Supplementary Information

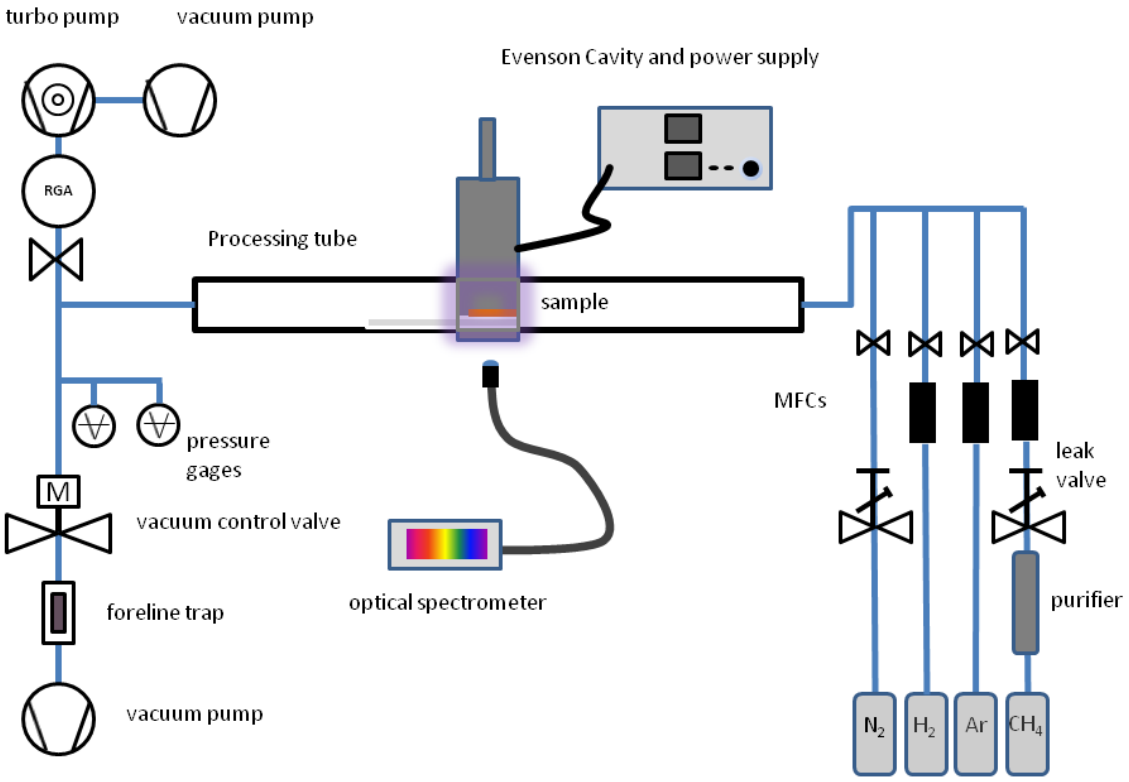

Supplementary Figure 1. A schematic of the experimental setup used for graphene fabrication.

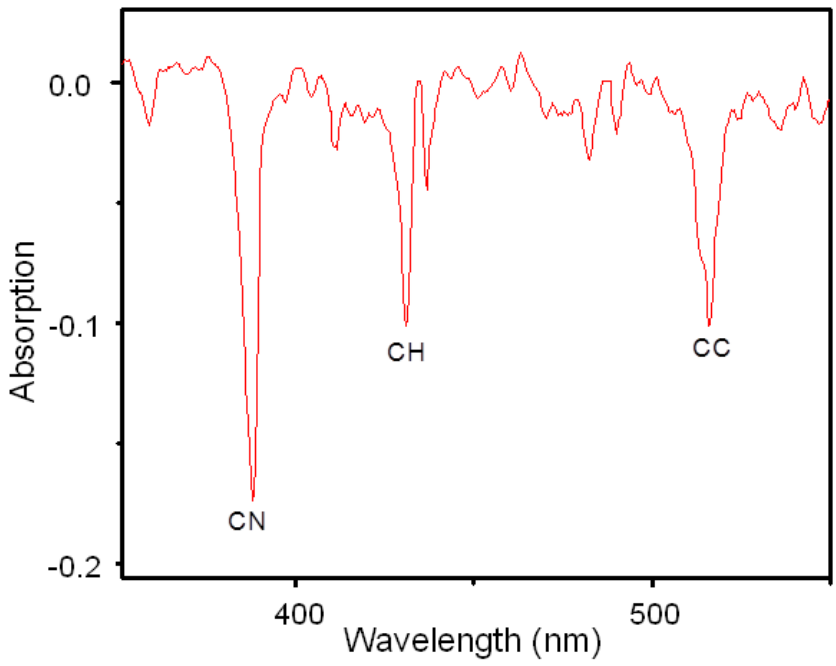

Supplementary Figure 2. Emission spectrum of the plasma: Negative peaks indicate an increase in particular species while positive peaks indicate a decrease.

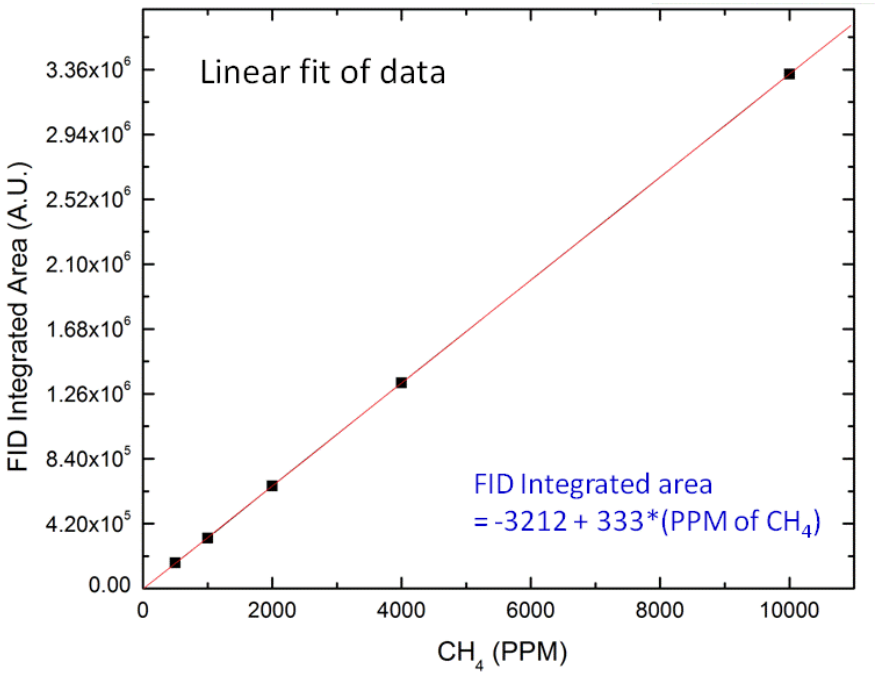

Supplementary Figure 3. Response of the FID detector to methane in nitrogen: The data are shown in units of PPM, and the line is a linear fit of the FID integrated area.

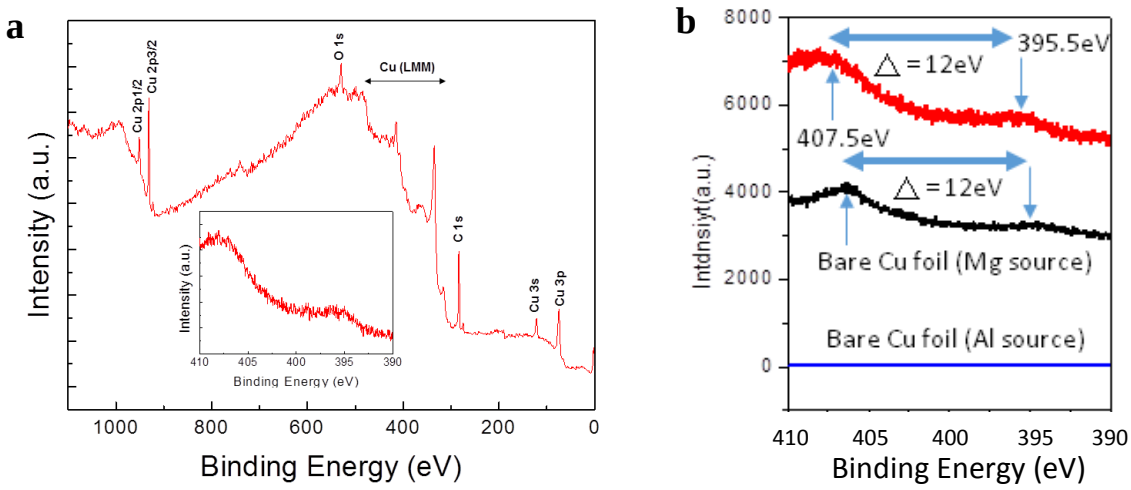

Supplementary Figure 4. XPS studies of PECVD-graphene on Cu: (**a**) XPS spectrum of a PECVD-graphene sample on Cu foil, showing no discernible signals at the N 1s core level binding energy (398.1eV). (**b**) Further investigation of two small peaks at 407.5 eV (Peak A) and 395.5 eV (Peak B) are attributed to the Auger lines of underlying Cu, as manifested by the consistent XPS spectral features for a bare Cu foil (black curve) with those of our graphene sample on Cu (red curve). The shifting in energy of the two peaks with changing the source of XPS from Mg to Al (blue curve) further support the fact that the peaks are from the Auger lines of Cu rather than the nitrogen 1s core level because the binding energy of nitrogen is independent of the x-ray energy.

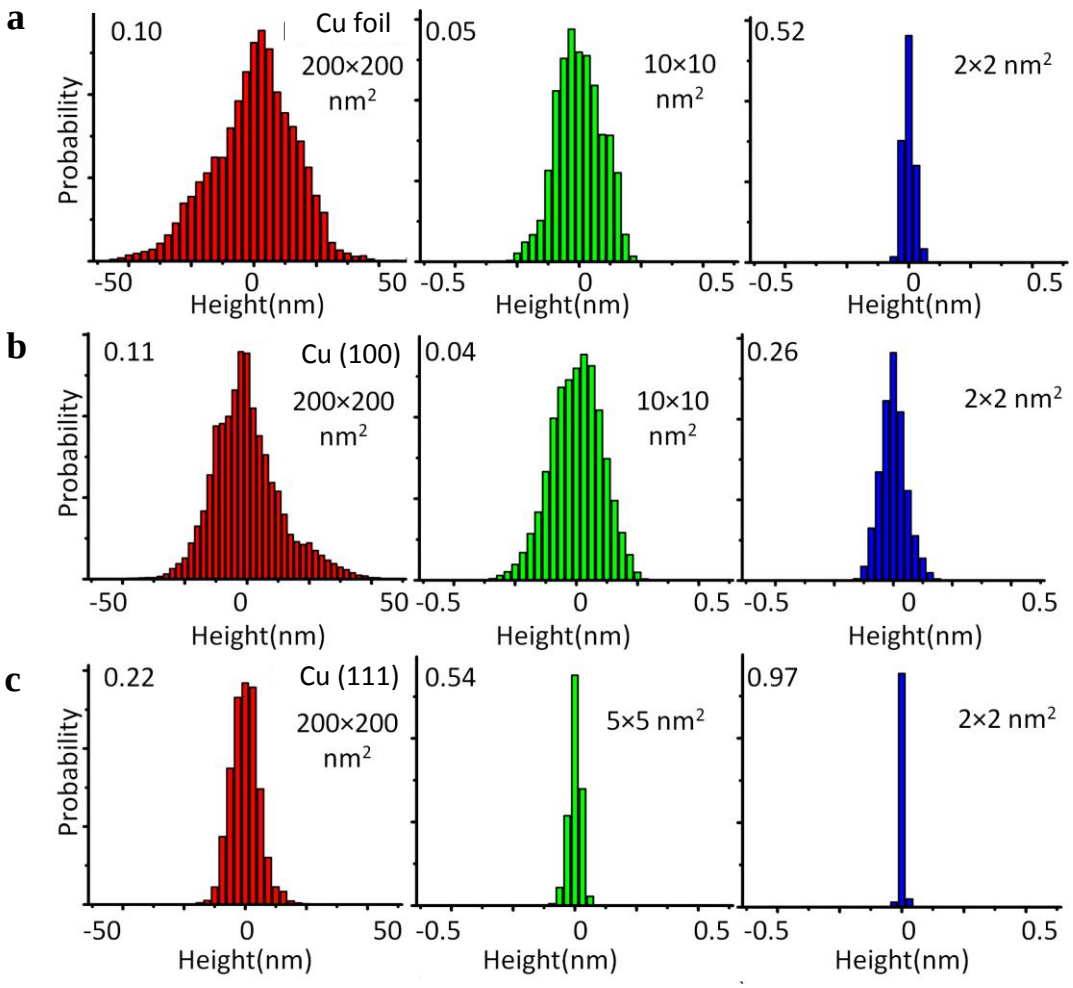

Supplementary Figure 5. STM studies of the surface morphology of PECVD-graphene on different substrates: From left to right, the height histograms of successively decreasing areas for PECVD-graphene on (**a**) Cu foil; (**b**) Cu (100) single crystal; and (**c**) Cu (111) single crystal. The overall surface morphology for PECVD-grown graphene appears to be much smoother than that of the 1000 °C thermal CVD-grown graphene at all length scales.

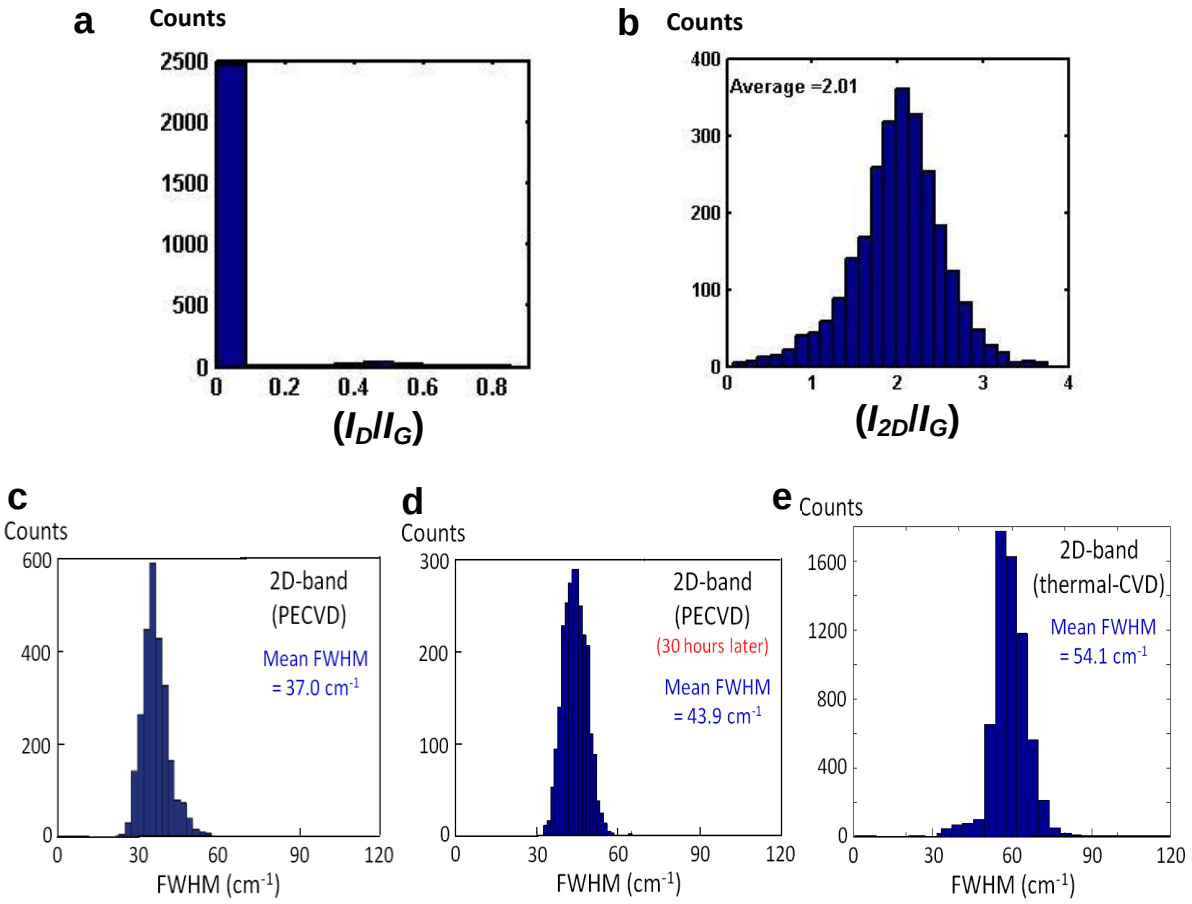

Supplementary Figure 6. Raman spectral analysis of PECVD-graphene on Cu: (a) Histogram of the *D*/*G* intensity ratios (I_D/I_G) of the Raman map in Figure 2b, showing nearly complete absence of the *D*-band signal (which is associated with defects) in the PECVD-grown graphene. (b) Histogram of the 2D/*G* intensity ratios (I_{2D}/I_G) of the Raman map in Figure 2b, showing the majority of the ratios exceeding 1, which is a figure of merit for the quality of monolayer graphene. (c) Histogram of the 2D-band linewidth (FWHM) of the same PECVD-graphene on Cu taken several days after growth, showing a mean FWHM = 37.0 cm^{-1}. (d) Histogram of the 2D-band FWHM of the same sample as in (c) taken at 30 hours later while continuously exposed to atmosphere, showing a mean FWHM = 43.9 cm^{-1}. (e) A comparative histogram of the 2D-band FWHM of a commercially purchased thermal-CVD grown graphene on Cu (Graphene Supermarket), showing a mean FWHM = 54.1 cm^{-1}.

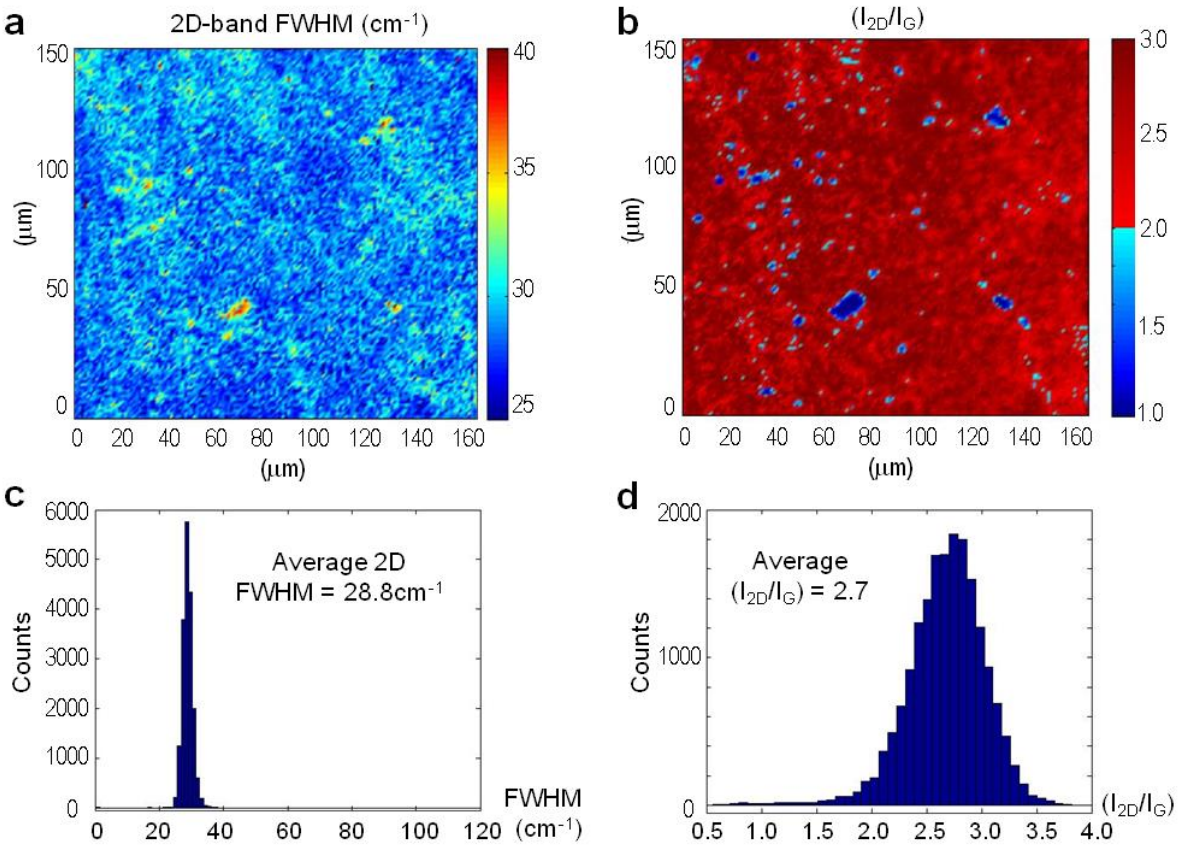

Supplementary Figure 7. Raman spectral analysis of PECVD-graphene transferred from Cu to SiO_2 after one year of its growth: (a) Spatial map of the FWHM of the 2D-band over an area of (160×150) μm^2, showing typical FWHM values < 30 cm^{-1}, which is a figure of merit for monolayer graphene according to S. Lee *et al.*, Nano Lett. **10,** 4702 (2010). (b) Spatial map of the 2D/*G* intensity ratios (I_{2D}/I_G) over the same sample area of as in (a), showing (I_{2D}/I_G) > 2 over most of the sample, again consistent with the figure of merit (I_{2D}/I_G) > 1 for monolayer graphene. (c) Histogram of the FWHM of the 2D-band in (a), showing a mean FWHM = 28.8 cm^{-1}. (d) Histogram of the 2D/*G* intensity ratios (I_{2D}/I_G) in (b), showing a mean value of (I_{2D}/I_G) = 2.7.

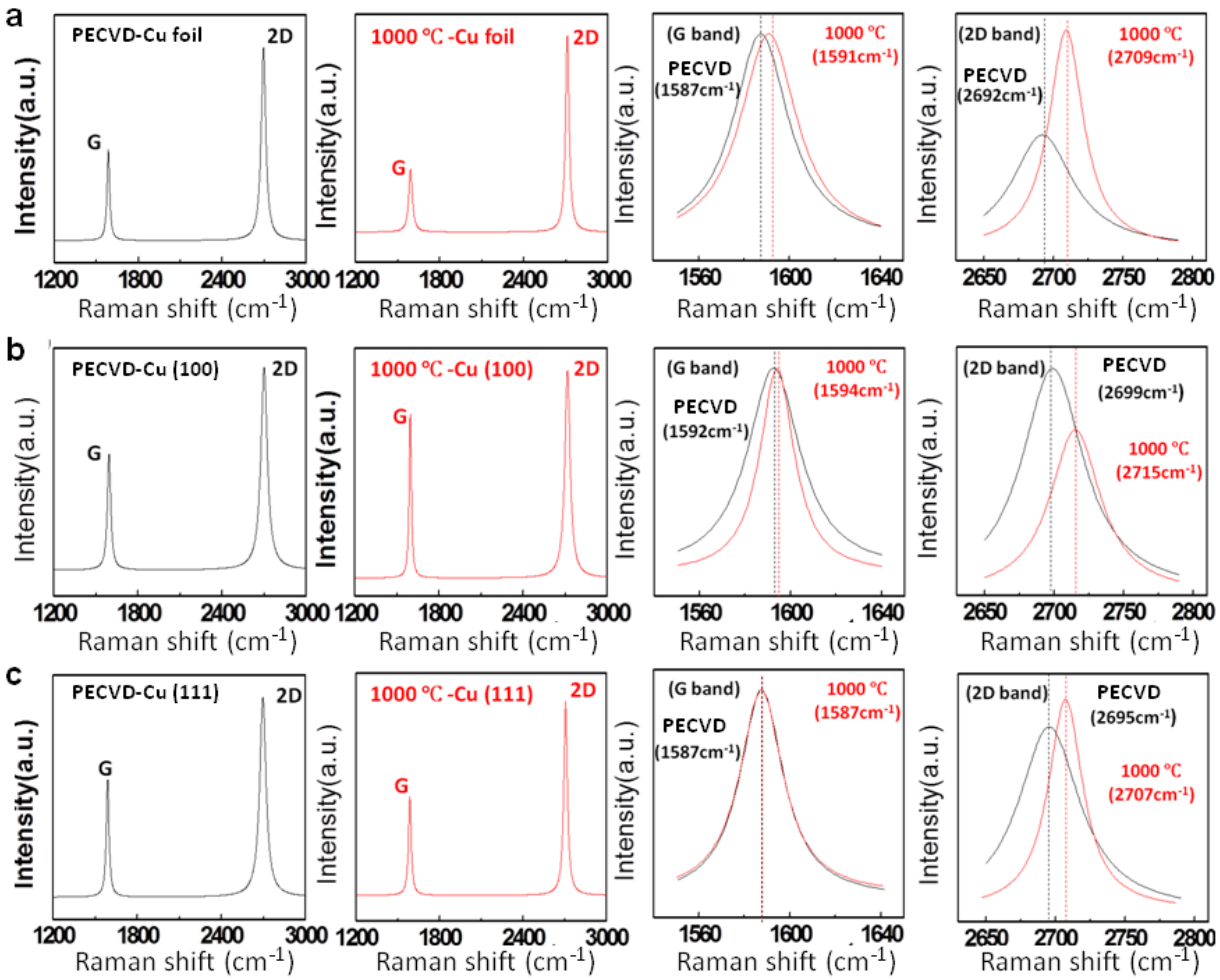

Supplementary Figure 8. Comparison of the Raman spectroscopy of PECVD-graphene and thermal CVD-grown graphene on different substrates: From left to right, Raman spectra of PECVD-graphene, 1000 °C-grown graphene, comparison of the 2D-band peaks, and comparison of the zone-centre G-band peaks for samples grown on (a) Cu foils, (b) Cu (100) and (c) Cu (111). The Raman spectra taken here were collected with a Renishaw M1000 @ 514 nm.

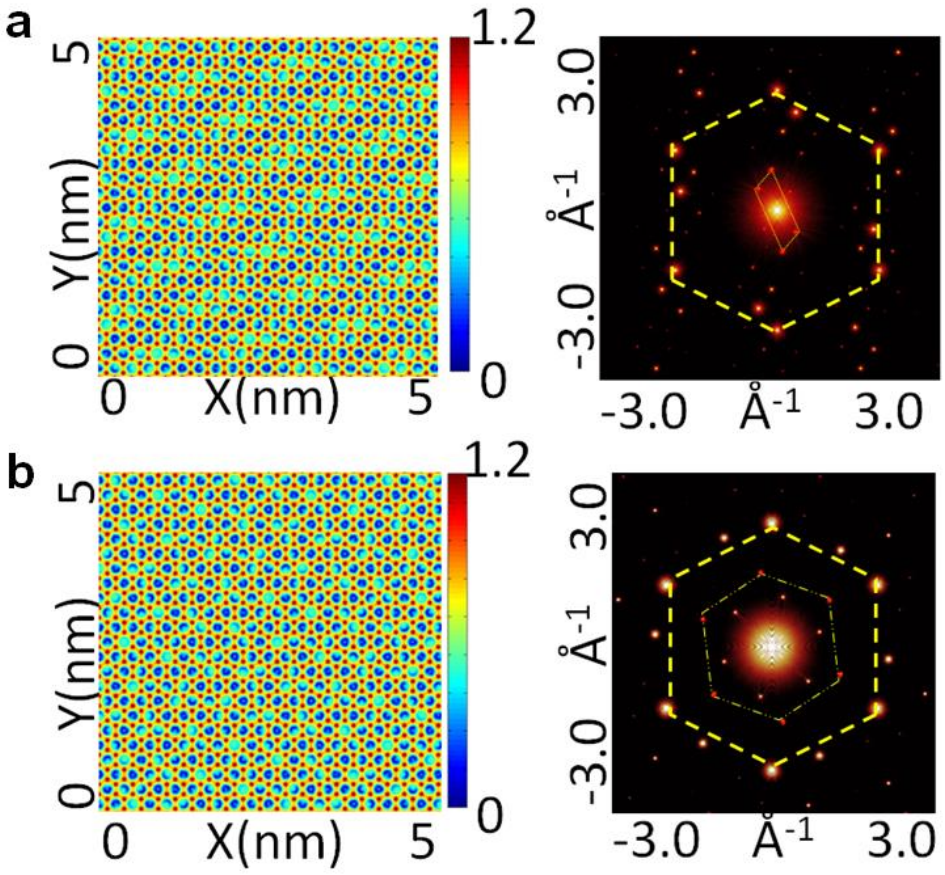

Supplementary Figure 9. Simulations of the real-space Moiré patterns (left panels) and the corresponding FT (right panels) for the 2D graphene honeycomb lattice on (a) Cu (100) square lattice and (b) Cu (111) hexagonal lattice. The FT Moiré pattern for graphene on Cu (100) is consistent with a honeycomb lattice at $\theta = (12\pm2)°$ relative to the square lattice of Cu (100), whereas that for graphene on Cu (111) is consistent with a honeycomb lattice at $\theta = (6\pm2)°$ relative to the hexagonal lattice of Cu (111). The FT Moiré patterns of **a,** and **b,** compare favorably with the FT spectra of Fig. 3b and Fig. 3c, respectively.

Supplementary Notes:

1. Analysis of the plasma in PECVD growth

The optical emission spectra (OES) of the plasma were measured using a fiber coupled spectrometer (S2000, Ocean Optics, Inc) placed directly below the Evenson cavity. Absorption spectra were taken prior to graphene deposition away from the area of the copper sample. The spectra were referenced to a pure hydrogen plasma, *i.e.*, before the addition of the flow of methane. Shown in Supplementary Figure 2 is a typical emission spectrum featuring CN (388 nm), CH (431 nm), and CC (516 nm),[1] where negative absorption peaks indicate an increase in a component and positive peaks indicate a decrease.

Graphene growth was performed on a variety of copper substrates, including high purity copper foil, common OFHC sheet, single crystal (100), and single crystal (111). Gas chromatography was used to measure the amount of methane in the hydrogen stream during graphene growth. The gas chromatograph (GC) was an HP 5890 II employing a flame ionization detector (FID). The FID was calibrated using reference standards (Mesa Gass, Inc) of 500, 1000, 2000, 4000, and 10000 ppm of CH_4 in nitrogen. The response (integrated peak area) of the FID to methane was found to be linear and is shown in Supplementary Figure 3.

Based on our investigations, we believe that the most likely plasma species acting upon Cu during the PECVD graphene growth are atomic hydrogen and CN radicals. Atomic hydrogen via a hydrogen plasma is known to be effective for removing native atmospheric derived species including Cu_2O, CuO, $Cu(OH)_2$, and $CuCO_3$. It has been recently reported that CN radicals can be highly reactive towards removing Cu from a semiconductor at room temperature.[2] Our overall observation of the PECVD graphene growth was in agreement with this notion. As an example, we increased the amount of nitrogen present in the system slightly and found that the PECVD growth could occur at half the normal plasma power. Conversely, under excess methane conditions the Cu substrate would not etch at even more than double the normal plasma power. The presence of both atomic hydrogen and CN species in the plasma could allow simultaneous preparation of the copper surface and deposition of high quality graphene at reduced temperatures. However, more experimental work will be necessary to fully understand the role of each radical plays in the growth process even though reproducible PECVD-growth without any active heating has been made.

While the presence of trace nitrogen in the plasma was essential for successful PECVD growth, we note that nitrogen was not incorporated into our PECVD-graphene, as verified by the studies of x-ray photoemission spectroscopy (XPS) in Supplementary figure 4a, where no discernible N 1s core level binding energy at 398.1eV could be resolved for a sample of monolayer graphene on Cu foil. We further note that the two small peaks at 407.5 eV (Peak A) and 395.5 eV (Peak B) are associated with the Auger lines of the Cu substrate rather than the nitrogen 1s core level in the graphene sample. This realization was achieved by comparing the XPS spectrum of a bare Cu foil as the control sample. As demonstrated in Supplementary Figure 4b, the XPS data obtained from the control sample (pure Cu foil) over the same energy range (black curve) are essentially identical to that of our graphene sample (red curve). Moreover, when the XPS source was changed from Mg to Al, Peak A and Peak B both disappeared,

indicating that they must be Auger lines of the underlying Cu substrate and that there was no nitrogen present in our graphene sample, because the nitrogen binding energy cannot be dependent on the x-ray energy.

2. Substrate influence on the Raman spectra of graphene

While the 2D-band FWHM of graphene may be used for analyzing whether a graphene sample consists of monolayer or multi-layers, possible changing properties of the underlying substrate could lead to complications in interpreting the Raman spectroscopic data. For instance, the 2D-band FWHM of our PECVD-grown graphene on Cu immediately after growth was ~ 29 cm^{-1}, which increased with time after growth and exposure to air, as exemplified in Supplementary Figure 6c-d. Similarly broadened FWHM of the 2D-band (Supplementary Figure 6e) was also observed in a commercial monolayer graphene sample on copper (from Graphene Supermarket) grown by the thermal CVD method. These findings are consistent with oxidation of the underlying Cu substrate, as discussed by Yin *et al*.[3]

The oxidation of the Cu substrate for our PECVD-graphene is likely the result of plasma-induced damages to the top side of Cu during the graphene growth. On the other hand, the quality of our PECVD-graphene remains intact despite the oxidation of the underlying Cu substrate, which has been verified by Raman spectroscopic studies of one of the PECVD-graphene samples transferred from Cu to SiO_2 after approximately one year of its growth. As demonstrated in Supplementary Figure 7a-d, a large spatial map of the sample over an area of (160×150) μm^2 reveals a mean FWHM = 28.8 cm^{-1} for the 2D-band and a mean 2D/G intensity ratio (I_{2D}/I_G) = 2.7, both are consistent with predominantly monolayer graphene if we use either the criterion FWHM < 30 cm^{-1} for the 2D-band as the figure of merit for monolayer graphene on SiO_2,[4] or the criterion (I_{2D}/I_G) > 1 for monolayer graphene on various substrates.[5,6,7,8] We further note the apparent correlation between the spatial maps of Supplementary Figure 7a-b, suggesting the consistency for determining monolayer graphene by using either the criterion for the FWHM of the 2D-band or that for the intensity ratio (I_{2D}/I_G).

Supplementary References:

1. Chatei, H. Bougdira, J. Rémy, M. Alnot, P. Bruch, C. Krüger, J. K. Effect of nitrogen concentration on plasma reactivity and diamond growth in a H_2-CH_4-N_2 microwave discharge. *Diamond and Related Materials* **6**, 107-119 (1997).
2. For patent information, see the website http://www.faqs.org/patents/app/20130017672.
3. Yin, X. *et al*. Evolution of the Raman spectrum of graphene grown on copper upon oxidation of the substrate. *Nano Research*, 1-10 (2014); doi:10.1007/s12274-014-0521-0.
4. Lee, S. *et al.* Wafer scale homogeneous bilayer graphene films by chemical vapor deposition. *Nano Lett.* **10,** 4702 (2010).
5. Ferrari, A. C. *et al.* Raman spectrum of graphene and graphene layers. *Phys. Rev. Lett.* **97**, 187401 (2006).
6. Wu, W. *et al*. Control of thickness uniformity and grain size in graphene films for transparent conductive electrodes. *Nanotechnology* **23**, 035603 (2012).
7. Dimiev, A. *et al.* Layer-by-layer removal of graphene for device patterning. *Science* **331**, 1168 (2011).
8. Zhou, H. *et al*. Chemical vapour deposition growth of large single crystals of monolayer and bilayer graphene. *Nature Communications* **4**, Article number: 3096.